

MDPI

Article

# **Experimental Approaches to Improve Yerba Mate Tissue Culture Using Nanoparticles**

Bruna Zanatta Pereira 1,\*0, Regina Caetano Quisen 2, Juliana Degenhardt 2 and Ivar Wendling 20

- Graduate Program in Forest Engineering, Federal University of Paraná (UFPR), Curitiba 80210-170, Paraná, Brazil
- Embrapa Forestry, Colombo 83411-000, Paraná, Brazil; regina.quisen@embrapa.br (R.C.Q.); juliana.degenhardt@embrapa.br (J.D.); ivar.wendling@embrapa.br (I.W.)
- \* Correspondence: brunazanattapereira@outlook.com

#### **Abstract**

Ilex paraguariensis (yerba mate), a culturally and economically important South American species, faces significant challenges in vitro, including contamination, phenolic oxidation, and low regeneration rates. Nanoparticles have recently emerged as promising tools to overcome such limitations. This study evaluated silver (AgNPs) and chitosan nanoparticles (ChNPs) in eight experiments using nodal, leaf, and internodal explants. Surface disinfection with 1% colloidal silver solution 20 ppm significantly reduced contamination (17.2% and 15%) while maintaining viability (62.1%). However, supplementation of culture media with AgNPs (4–75 mg·L<sup>-1</sup>) or ChNPs (5–120 mg·L<sup>-1</sup>) did not improve nodal segment responses. In leaf explants, 4 mg·L<sup>-1</sup> AgNPs proved most effective, reducing contamination and markedly decreasing callus oxidation from 63.3% to 10.0%. Callogenesis was enhanced when AgNPs were combined with growth regulators, with the highest induction at 6 mg·L $^{-1}$  AgNPs + zeatin (38.1%) and 4 mg·L $^{-1}$  AgNPs + BAP (42.9%). Conversely, in internodal segments, AgNPs combined with BAP completely inhibiting callus formation. The resulting calli exhibited compact and friable morphologies but no signs of somatic embryogenesis. Overall, the effectiveness of AgNPs depends on their formulation, explant type, and interaction with cytokinins. Optimization of nanoparticle formulation and hormonal balance remains essential to maximize efficacy while minimizing toxicity.

Keywords: Ilex paraguariensis; silver nanoparticles; chitosan nanoparticles; tissue culture



Academic Editors: Marcos Edel Martinez-Montero and Judit Dobránszki

Received: 31 July 2025 Revised: 29 August 2025 Accepted: 1 September 2025 Published: 6 September 2025

Citation: Pereira, B.Z.; Quisen, R.C.; Degenhardt, J.; Wendling, I. Experimental Approaches to Improve Yerba Mate Tissue Culture Using Nanoparticles. *Forests* **2025**, *16*, 1429. https://doi.org/10.3390/f16091429

Copyright: © 2025 by the authors. Licensee MDPI, Basel, Switzerland. This article is an open access article distributed under the terms and conditions of the Creative Commons Attribution (CC BY) license (https://creativecommons.org/licenses/by/4.0/).

# 1. Introduction

*Ilex paraguariensis* A. St.-Hil., commonly known as yerba mate, is a tree species of the family Aquifoliaceae with great economic, cultural, and ecological importance in South America. It is widely cultivated in agroforestry systems and commercial monocultures across Brazil, Argentina, and Paraguay [1,2]. In addition to its traditional use in infusions such as chimarrão and tereré, yerba mate has gained prominence in the international markets of functional foods, cosmetics, and nutraceuticals, driven by its rich phytochemical profile. The leaves contain methylxanthine alkaloids, phenolic acids, flavonoids, and triterpene saponins, which exhibit antioxidant, anti-inflammatory, digestive, neuroprotective, and lipid-lowering properties [3,4].

The growing demand for high-quality, genetically uniform plantlets has prompted the development of vegetative propagation techniques. Techniques such as cuttings and mini-cuttings are among the most widely used [5–8]. However, their success depends not

Forests 2025, 16, 1429 2 of 18

only on morphological traits but also on the physiological and biochemical status of the propagules. The metabolic condition of the donor plant (strongly influenced by genotype and seasonality) plays a decisive role in rooting and subsequent development [7,8].

In vitro culture techniques, on the other hand, overcome seasonal constraints, ensure genetic and physiological uniformity, provide high phytosanitary quality, and enable large-scale production [9,10]. Nevertheless, the micropropagation of yerba mate still faces several technical limitations. These include persistent endogenous contamination caused by endophytes that survive surface sterilization [11,12]; severe explant oxidation, where released phenolic compounds oxidize into toxins causing tissue necrosis [13], and the inherently low regenerative capacity of mature genotypes, which remain recalcitrant to growth regulators due to physiological maturity [14,15].

To address these challenges, innovative biotechnological strategies such as the application of nanoparticles have been explored in several plant species, including, potato (*Solanum tuberosum* L.) [16], sugarcane (*Saccharum* spp.) [17], strawberry (*Fragaria* × *ananassa* Duchesne ex Rozier) [18], *Lavandula angustifolia* Mill. [19], and *Araucaria excelsa* (Lamb.) R. Sm. [20]. These studies report that silver (AgNPs) and chitosan nanoparticles (ChNPs) can enhance in vitro culture efficiency by exerting antimicrobial and antioxidant effects, thereby reducing contamination and, in some cases, promoting shoot formation and callogenesis.

The selection of AgNPs and ChNPs in the present study was based on their well-documented antimicrobial activity and their potential role as plant growth elicitors. Mechanistically, AgNPs interact with microbial cell membranes and promote the formation of reactive oxygen species, disrupting essential cellular functions [21]. ChNPs, in turn, establish electrostatic interactions with microbial membranes and chelate metal ions, leading to cell wall damage and growth inhibition [22]. Nonetheless, the biological effects of nanoparticles are highly variable and depend on species-specific and explant-specific factors, including nanoparticle type, concentration, exposure time, and colloidal stability [23].

Despite increasing interest in the subject, this is the first study to evaluate the effectiveness of nanoparticles in the in vitro regeneration of yerba mate. Given the well-known challenges of contamination, oxidation, and regeneration in this species, the use of nanotechnology represents a promising and still underexplored alternative that could provide significant scientific contributions to the field of plant tissue culture.

Therefore, this study aimed to evaluate the effects of silver (AgNPs), and chitosan nanoparticles (ChNPs) at different concentrations on the disinfection, shoot induction, and callus formation of nodal, foliar and internodal explants of yerba mate, to optimize tissue culture protocols. By integrating classical techniques with emerging nanobiotechnological approaches, this work also aimed to contribute to the development of more efficient and reproducible methods for clonal propagation and germplasm conservation of yerba mate.

#### 2. Materials and Methods

# 2.1. Plant Material, Nanoparticles, and Experimental Design

Plants from clones of yerba mate were maintained in a semi-hydroponic minigarden located in a greenhouse at Embrapa Forestry (Colombo, Brazil). These plants were originated from a provenance and progeny trial established in 1997 in Ivaí, Paraná, Brazil, and propagated by cuttings from selected genotypes. At the time of rescue from the field, donor plants were 21 years old, and the clonal cuttings remained in the semi-hydroponic channels for five years before being used in the experiments. All experiments were conducted at the Tissue Culture and Transformation Laboratory, Embrapa Forestry, using plants from a mix of clones.

Forests 2025, 16, 1429 3 of 18

A total of eight independent experiments were performed on the effects of nanoparticles on various aspects of yerba mate in vitro culture. Three experiments assessed the effects of silver (AgNPs) and chitosan nanoparticles (ChNPs) on explant disinfection and shoot induction using nodal segments. The remaining five experiments employed leaf and internodal explants to investigate disinfection efficiency, oxidation control, silver nanoparticle dose–response effects, growth regulator exposure time, and callus induction and differentiation.

Silver nanoparticles were applied in two different form and at various concentrations: (i) a commercial colloidal silver solution 20 ppm (Universe Nanoscience, São José dos Campos, Brazil). The solution was characterized by a light yellow to amber color and a slightly bitter taste. Transmission Electron Microscopy (TEM) analysis confirmed the presence of spherical nanoparticles with a bimodal size distribution, exhibiting average diameters of 8 nm and 30 nm; (ii) a silver nanopowder (Sigma-Aldrich®, St. Louis, MO, USA) with a particle size of <100 nm. The nanopowder contains Polyvinylpyrrolidone (PVP) as a dispersant agent and has a high purity of 99.5% (trace metals basis), presenting a beige to dark gray appearance.

Additionally, chitosan nanoparticles (ChNps) in nanopowder form (<30 nm) were kindly provided by Quitomax Indústria e Comércio Ltda. (Maripá, Brazil). Their production process and physicochemical characterization have been previously described in Alves et al., 2018, 2021 [24,25] and Oliveira et al., 2025 [26]

Experimental protocols were progressively refined based on previous outcomes to optimize each developmental stage.

#### 2.2. Explant Preparation and Surface Disinfection

Fresh nodal (1.0–1.5 cm long), leaf (1 cm² disk), and intermodal (0.5 cm long) segments were transported to the laboratory in an antioxidant solution (25 mg·L $^{-1}$  citric acid 250 mg·L $^{-1}$  ascorbic acid, and 1 g·L $^{-1}$  polyvinylpyrrolidone (PVP)) to minimize oxidative browning. Upon arrival, explants were rinsed under running water with detergent Tween® 20 (Sigma-Aldrich®, St. Louis, MO, USA) for 5 min.

Surface sterilization was performed by sequential immersion in 70% ethanol for 2 min, and then in 1.25% sodium hypochlorite (prepared as a 50% dilution of 2.5% stock solution) for 20 min with constant agitation. After each chemical treatment, explants were rinsed three times with sterile distilled water to remove residual disinfectants. The explants were then re-immersed in the antioxidant solution (same composition as above) until they inoculated onto culture media.

Supplementary disinfection protocols were evaluated in Experiment I (nodal segments) and Experiment IV (leaf and internodal segments). The most effective treatment from each experiments (see Tables 1 and 2 for details) was adopted as the standard sterilization procedure for subsequent work.

| Experiment                                      | Treatment  | Culture Medium  |  |
|---|--|---|--|
| Exp. I—Disinfection and Shoot Induction         | (I and IV) 1% Commercial colloidal silver solution 20 ppm for 20 min; (II and III) 0.2–2% Chlorhexidine for 10 min; (V) 1% Cercobin <sup>®</sup> (Ihara, Sorocaba, Brazil) for 15 min.   | $^{1}$ 2 MS + 30 g·L $^{-1}$ sucrose + 7 g·L $^{-1}$ agar + 2.22 μM BAP + 0.1 μM NAA + (II–V) 0.075% Coryna $^{\otimes}$ 116-XC (Miracema-Nuodex, Campinas, Brazil); pH 5.6–5.8 |  |
| Exp. II—Silver<br>and Chitosan<br>Nanoparticles | Culture media supplemented with: (I) $0 \text{ mg} \cdot \text{L}^{-1} \text{ NPs}$ ; (II) $4 \text{ mg} \cdot \text{L}^{-1} \text{ AgNPs}$ ; (III) $7 \text{ mg} \cdot \text{L}^{-1} \text{ AgNPs}$ ; (IV) $5 \text{ mg} \cdot \text{L}^{-1} \text{ ChNPs}$ ; (V) $15 \text{ mg} \cdot \text{L}^{-1} \text{ ChNPs}$ | $^{1/2}$ MS + 30 g·L $^{-1}$ sucrose + 7 g·L $^{-1}$ agar + 2.22 μM BAP + 0.1 μM NAA + 0.075% Coryna $^{®}$ 116-XC; pH 5.6–5.8  |  |

Forests 2025, 16, 1429 4 of 18

Table 1. Cont.

| Experiment                                       | Treatment   | Culture Medium |
|--|---|----------------|
| Exp. III—Silver<br>and Chitosan<br>Nanoparticles | Culture media supplemented with: (I) 25 mg·L $^{-1}$ AgNPs; (II) 50 mg·L $^{-1}$ AgNPs; (III) 75 mg·L $^{-1}$ AgNPs; (IV) 60 mg·L $^{-1}$ ChNPs; (V) 90 mg·L $^{-1}$ ChNPs; (VI) 120 mg·L $^{-1}$ ChNPs | Same as above  |

NAA (1-Naphthaleneacetic acid); BAP (6-Benzylaminopurine). For each experiment, 30 replicates were conducted per treatment.

Table 2. Summary of in vitro culture experiments on leaf and internodal segments of yerba mate.

| Experiment   | Explant<br>Type  | Treatment Applied   | Culture Media  | Evaluated<br>Variables   |
|--|--|---|--|--|
| Exp. IV— Disinfection  | $ \begin{array}{c ccccccccccccccccccccccccccccccccccc$ |   | $^{1/2}$ MS + 30 g·L $^{-1}$ sucrose + 7 g·L $^{-1}$ agar + 2.22 μM BAP + 0.1 μM NAA + 0.075% Coryna $^{\circledR}$ 116-XC; pH 5.5   | Contamination,<br>Oxidation,<br>Viability                          |
| Exp. V—ethylene-inhibiting and Callogenesis  |  |   | Modified MS ( $\frac{1}{2}$ NH <sub>4</sub> NO <sub>3</sub> and KNO <sub>3</sub> ) + 30 g·L <sup>-1</sup> sucrose + 7 g·L <sup>-1</sup> agar + 4.56 $\mu$ M zeatin + 4.53 $\mu$ M 2,4-D + 20 $\mu$ M ethylene-inhibiting; pH 5.5 | Contamination, Oxidation, Viability, Callogenesis, Callus Browning |
| $ \begin{array}{c} \text{Exp. VI}  \text{AgNPs} \\ \text{and Callogenesis} \end{array} \text{ Leaf} & \begin{array}{c} \text{(I) No AgNPs;} \\ \text{(II) 2 mg} \cdot \text{L}^{-1} \text{ AgNPs;} \\ \text{(III) 3 mg} \cdot \text{L}^{-1} \text{ AgNPs;} \\ \text{(IV) 4 mg} \cdot \text{L}^{-1} \text{ AgNPs;} \\ \text{(IV) 4 mg} \cdot \text{L}^{-1} \text{ AgNPs;} \\ \end{array} \\ \text{Exp. VII}  \text{AgNPs} \\ \text{and Callogenesis} \end{array} \text{ Leaf} & \begin{array}{c} \text{(I) No AgNPs;} \\ \text{(II) 4 mg} \cdot \text{L}^{-1}; \\ \text{(III) 8 mg} \cdot \text{L}^{-1}; \\ \text{(IV) 12 mg} \cdot \text{L}^{-1} \end{array} $ |  | (II) $2 \text{ mg} \cdot \text{L}^{-1} \text{ AgNPs}$ ;<br>(III) $3 \text{ mg} \cdot \text{L}^{-1} \text{ AgNPs}$ ;                       | $^{1/4}$ MS + 30 g·L $^{-1}$ sucrose + 7 g·L $^{-1}$ agar + 4.56 $\mu$ M zeatin + 4.53 $\mu$ M 2,4-D + 250 mg·L $^{-1}$ glutamine + AgNPs; pH 5.5  | Contamination, Oxidation, Viability, Callogenesis, Callus Browning |
|  |  | Same as above   | Contamination,<br>Oxidation,<br>Viability,<br>Callogenesis   |  |
| Exp. VIII—<br>Nanoparticles and<br>Growth Regulators   | Leaf and<br>Internodal                                 | (I–IV) AgNPs<br>(0, 4, 6, 8 mg·L <sup>-1</sup> ) +<br>ZEA 4.56 μM;<br>(V–VIII) AgNPs<br>(0, 4, 6, 8 mg·L <sup>-1</sup> ) +<br>BAP 4.44 μM | $^{1\!\!4}$ MS + 30 g·L $^{-1}$ sucrose + 7 g·L $^{-1}$ agar + 250 mg·L $^{-1}$ glutamine + 0.075% Coryna $^{\circledR}$ 116-XC + 4.5 $\mu$ M 2,4-D + respective cytokinin + AgNPs; pH 5.5                                       | Contamination,<br>Oxidation,<br>Viability,<br>Callogenesis         |

 $NAA \ (1-Naphthaleneacetic\ acid);\ BAP\ (6-Benzylaminopurine);\ ZEA\ (Zeatin).\ For\ each\ experiment,\ 30\ replicates$  were conducted per treatment.

#### 2.3. Culture Conditions and Evaluation

Basal media were prepared using Murashige and Skoog (MS) salts [27], with pH adjusted to either 5.8 or 5.5 before autoclaving at 121 °C for 20 min. Specific medium compositions for each experiment are detailed in Tables 1 and 2.

Cultures of nodal segments were maintained in darkness until sprouting, whereas leaf and internodal explants remained in darkness throughout the entire culture period. Incubation was conducted at 23  $\pm$  2 °C, under either complete darkness or a 16 h photoperiod with a light intensity of 40  $\mu mol \cdot m^{-2} \cdot s^{-1}$ , depending on the experimental objectives. Cultures were subcultured every three to four weeks.

Viability, contamination, oxidation, and, when applicable, shoot or callus formation were evaluated after 30 days. In some experiments, assessments were also performed after 60 or 90 days, depending on the design.

Forests 2025, 16, 1429 5 of 18

#### 2.4. Callus Differentiation

Calli induced from Experiment VI, VII and VIII were transferred to ¼ MS medium supplemented with 2,4-D (2.27 or 4.53  $\mu$ M), either BAP (8 or 16  $\mu$ M) or kinetin (8.5 or 17  $\mu$ M), glutamine (250 mg·L $^{-1}$ ), and 0.075% Coryna<sup>®</sup> 116-XC. The pH was adjusted to 5.5. Cultures were maintained in darkness at 25  $\pm$  2 °C.

#### 2.5. Callus Morphological Characterization

Callus friability was visually assessed based on texture and ease of fragmentation, while callus color was categorized according to predominant pigmentation. Morphological characteristics of the callus were evaluated using a Ivesta 3 stereoscopic microscope (Leica Microsystems, Wetzlar, Germany). The analysis focused on assessing callus texture (friability), and general morphology, including shape and color.

# 2.6. Characterization of Silver Nanoparticle Nanopowder (Sigma-Aldrich®) and Chitosan Nanoparticle Nanopowder

Silver and chitosan nanoparticles were characterized using physicochemical and morphological techniques. Hydrodynamic diameter, polydispersity index (PDI), and zeta potential were determined using a Zetasizer Nano ZS instrument (Malvern Panalytical, Malvern, UK) employing dynamic light scattering (DLS) and electrophoretic mobility techniques at Biopolymers Laboratory, Federal University of Paraná (UFPR). Analyses were performed at 25 °C with a detection angle of 173° after diluting the samples in ultrapure Milli-Q water (Merck Millipore, Darmstadt, Germany). The PDI provided information on particle size homogeneity, while zeta potential was used to evaluate the colloidal stability.

Morphological analysis was conducted by scanning electron microscopy (SEM), using a MIRA3 instrument (Tescan, Brno, Czech Republic) at Electron Microscopy Center, Federal University of Paraná. Samples were prepared by deposition onto metal stubs with conductive copper tape and dried at room temperature. Chitosan samples were sputter-coated with a thin gold layer to ensure electrical conductivity, while silver samples were analyzed without coating. The obtained images allowed observation of particle shape, distribution, and potential aggregation, complementing the DLS data.

#### 2.7. Statistical Analysis

All response variables were binary, representing the proportion of explants exhibiting specific physiological or sanitary outcomes (contamination, oxidation, viability, shoot formation, or callogenesis). Generalized Linear Models (GLMs) with a binomial distribution and logit link function were fitted to analyze these data [28]. When significant treatment effects were detected, planned orthogonal contrasts were applied to compare specific groups [29]. Logistic regression with Firth's correction was applied across all experiments due to data separation, where some treatments presented very low or zero frequencies. This approach provides more stable estimates in the presence of rare events [30], with models fitted using R software (v4.4.2, R Core Team, 2024).

Odds ratios (ORs) and their corresponding 95% confidence intervals (CI 95%) were estimated to quantify the magnitude and direction of treatment effects relative to controls [31]. Observed response frequencies were also considered to support biological interpretation. Significance letters were assigned based on: (i) orthogonal contrasts results (p < 0.05); (ii) odds ratios compared to the control group; and (iii) inclusion or exclusion of the null value (OR = 1) in the confidence intervals. Treatments that did not differ significantly and had overlapping 95% confidence intervals were grouped under the same letter [32]. This approach integrated statistical significance and biological relevance in a clear, interpretable manner. All statistical analyses were performed using R version 4.4.2 [33].

Forests 2025, 16, 1429 6 of 18

#### 2.8. Use of Generative AI

Generative AI tools (ChatGPT, OpenAI) were used solely for language editing and improving readability of certain sections in this manuscript. The AI was not employed for data analysis, interpretation, or generating any original content. All statistical methods, results, and conclusions remain entirely human-authored and validated. The use of AI was supervised by the authors, who take full responsibility for the final content.

#### 3. Results

#### 3.1. Disinfection Treatments in Nodal Segments (Experiment I)

After 30 days of culture, the disinfection treatments significantly affected explant contamination ( $\chi^2=24.65;\ p<0.001;$  Table 3). The application of 1% colloidal silver solution 20 ppm and chlorhexidine (0.2% and 2%) significantly reduced contamination compared to the control (p<0.0001). For oxidation ( $\chi^2=19.60;\ p<0.001$ ), the fungicide (1% of Cercobin®) treatment led to a significant increase (70%). Regarding explant viability ( $\chi^2=37.29;\ p<0.001$ ), the best results were obtained with 1% of colloidal silver solution 20 ppm and chlorhexidine (0.2 and 2%) with 43% to 62% viable explants, in contrast to the poor performance observed in the control. No significant differences were observed among treatments for shoot formation ( $\chi^2=6.42;\ p=0.093$ ), suggesting that the disinfection protocols did not directly affect shoot induction.

**Table 3.** Effects of different disinfection treatments on contamination, oxidation, viability, and shoot formation in nodal segments of yerba mate after 30 days of in vitro culture (Exp. I).

| Treatment                           | Contamination (%) | Oxidized (%) | Viable (%) | Shoots 'ns' (%) |
|-------------------------------------|-------------------|--------------|------------|-----------------|
| Control                             | 73.30 b           | 36.70 a      | 10.00 b    | 10.00           |
| Chlorhexidine 0.2%                  | 23.30 a           | 27.30 a      | 60.00 a    | 36.70           |
| Chlorhexidine 2%                    | 33.30 a           | 36.70 a      | 43.30 a    | 20.00           |
| Colloidal Silver Solution 20 ppm 1% | 17.20 a           | 20.70 a      | 62.10 a    | 20.70           |
| Fungicide (Cercobin®) 1%            | 40.00 a           | 70.00 b      | 10.00 b    | 0.00            |

Orthogonal comparisons among treatments. Different letters indicate significant differences (p < 0.05) based on adjusted orthogonal contrast tests. Odds ratios and standard error values provided in Supplementary Materials. 'ns'—not statistically different.

# 3.2. Effect of Nanoparticles on Shoot Induction from Nodal Segments (Experiment II and III)

The treatments with silver nanoparticles (AgNPs) and chitosan nanoparticles (ChNPs) tested in the Exp. II negatively affected contamination ( $\chi^2 = 22.45$ ; p < 0.001) and explant viability ( $\chi^2 = 25.58$ ; p < 0.001) (Table 4). Regarding viability, both AgNPs and ChNPs treatments significantly reduced the proportion of viable explants.

In the second experiment (Exp. III), which evaluated higher concentrations of AgNPs and ChNPs, no significant effects were observed on contamination ( $\chi^2 = 9.11$ ; p = 0.105), viability ( $\chi^2 = 3.70$ ; p = 0.593), or shoot formation ( $\chi^2 = 3.54$ ; p = 0.617) after 60 days of culture. The results showed contamination up to 30%, oxidation close to 67%, and viability not exceeding 38% (Table 5). Phytotoxicity in the explants was manifested by loss of vigor and darkening of both the bud and the stem see in Figure 1.

Forests 2025, 16, 1429 7 of 18

| Table 4. Effects of silver (AgNPs) and chitosan nanoparticles (ChNPs) on contamination, oxidation           |
|---|
| viability, and shoot formation in nodal segments of yerba mate after 30 days of in vitro culture (Exp. II). |

| Treatment   | Contamination (%) | Oxidized (%) 'ns' | Viable (%) | Shoots (%) 'ns' |
|---|-------------------|-------------------|------------|-----------------|
| Control   | 30.00 a           | 23.30             | 66.70 a    | 13.30           |
| $4 \text{ mg} \cdot \text{L}^{-1} \text{ AgNPs}$  | 76.70 b           | 56.70             | 13.30 с    | 0.30            |
| $7 \text{ mg} \cdot \text{L}^{-1} \text{ AgNPs}$  | 63.30 b           | 46.70             | 33.30 bc   | 0.00            |
| $5 \text{ mg} \cdot \text{L}^{-1} \text{ ChNps}$  | 83.30 b           | 50.00             | 16.70 bc   | 6.70            |
| $15 \text{ mg} \cdot \text{L}^{-1} \text{ ChNps}$ | 56.70 b           | 50.00             | 43.30 b    | 10.00           |

Orthogonal comparisons among treatments. Different letters indicate significant differences (p < 0.05) based on adjusted orthogonal contrast tests. Odds ratios and standard error values provided in Supplementary Materials. 'ns'—not statistically different.

**Table 5.** Effects of silver (AgNPs) and chitosan nanoparticles (ChNPs) nodal segments of yerba mate after 60 days of in vitro culture (Exp. III).

| Treatment  | Contamination (%) 'ns' | Oxidized (%) 'ns' | Viable (%) 'ns' | Shoots (%) 'ns' |
|--|------------------------|-------------------|-----------------|-----------------|
| 25 mg⋅L <sup>-1</sup> AgNps                        | 30.00                  | 60.00             | 23.30           | 33.30           |
| $50 \text{ mg} \cdot \text{L}^{-1} \text{ AgNps}$  | 33.30                  | 66.70             | 16.70           | 20.00           |
| $75 \text{ mg} \cdot \text{L}^{-1} \text{ AgNps}$  | 13.30                  | 43.30             | 16.70           | 26.70           |
| $60 \text{ mg} \cdot \text{L}^{-1} \text{ ChNps}$  | 26.70                  | 40.00             | 26.70           | 23.30           |
| $90 \text{ mg} \cdot \text{L}^{-1} \text{ ChNps}$  | 10.00                  | 40.00             | 23.30           | 36.70           |
| $120 \text{ mg} \cdot \text{L}^{-1} \text{ ChNps}$ | 13.80                  | 51.70             | 37.90           | 20.70           |

Odds ratios provided in Supplementary Materials 'ns'—not statistically different.



**Figure 1.** Representative image of visible symptoms of phytotoxicity observed in the explants exposed to higher concentrations of nanoparticles.

# 3.3. Disinfection in Leaf Explants (Experiment IV)

Disinfection treatments had a significant effect on contamination ( $\chi^2 = 17.31$ ; p < 0.001) and oxidation ( $\chi^2 = 9.01$ ; p = 0.029) (Table 6). The 20 min commercial coloidal silver solution 20 ppm treatment significantly reduced both contamination and oxidation compared to the other protocols. In contrast, the 10 min exposure to commercial coloidal silver solution 20 ppm proved less effective, with statistically significant differences observed between the two exposure durations. The remaining treatments showed intermediate results, with no significant differences among them.

Forests 2025, 16, 1429 8 of 18

| Table 6. Effect of different disinfection treatments on contamination and oxidation of leaf explants of |
|---|
| yerba mate after 30 days of in vitro culture (exp. IV).   |

| Treatment                                  | Contamination (%) | Oxidized (%) |
|--|-------------------|--------------|
| Sodium hypochlorite 1.25% 10 min.          | 65.00 b           | 75.00 b      |
| Sodium hypochlorite 1.25% 20 min.          | 35.00 ab          | 60.00 b      |
| Colloidal Silver Solution 20 ppm 1%10 min  | 70.00 b           | 75.00 b      |
| Colloidal Silver Solution 20 ppm 1% 20 min | 15.00 a           | 35.00 a      |

Orthogonal comparisons among treatments. Different letters indicate significant differences (p < 0.05) based on adjusted orthogonal contrast tests. Odds ratios and standard error values provided in Supplementary Materials.

#### 3.4. Antioxidants in Leaf Explants (Experiment V)

After 90 days in vitro culture, no significant differences were observed among treatments for contamination ( $\chi^2 = 1.25$ ; p = 0.741), oxidation ( $\chi^2 = 1.27$ ; p = 0.737), explant viability ( $\chi^2 = 2.03$ ; p = 0.567), or callus induction ( $\chi^2 = 2.98$ ; p = 0.395), indicating that the disinfection protocols did not exert a statistically significant influence on these parameters. In contrast, callus browning differed significantly among groups ( $\chi^2 = 10.74$ ; p = 0.013), with the highest incidence observed in the control (20.70%). In the other treatments—silver nitrate (AgNO<sub>3</sub>); sodium thiosulfate (ST); silver thiosulfate (STS)—browning rates were considerably lower, ranging from 0 to 6.7%. Nevertheless, despite this apparent trend, the planned orthogonal contrasts did not detect statistically significant differences between treatments, likely due to the low overall frequency of oxidized calli, which resulted in high variance and limited the precision of model estimates (Table 7).

**Table 7.** Effect of different antioxidants in leaf explants of yerba mate after 90 days of in vitro culture (Exp. IV).

| Treatment | Contaminated (%) 'ns' | Oxidized (%) 'ns' | Viable (%) 'ns' | Callus (%) 'ns' | Oxidized Callus (%) 'ns' |
|-----------|-----------------------|-------------------|-----------------|-----------------|--------------------------|
| Control   | 24.10                 | 31.00             | 69.00           | 79.30           | 20.70                    |
| $AgNO_3$  | 26.70                 | 40.00             | 60.00           | 66.70           | 3.30                     |
| ST        | 30.00                 | 43.30             | 53.30           | 63.30           | 0.00                     |
| STS       | 36.70                 | 43.30             | 53.30           | 60.00           | 6.70                     |

Odds ratios provided in Supplementary Materials. 'ns'—not statistically different.

# 3.5. Effect of AgNPs Concentrations in Leaf Explants Callogenesis (Experiment VI and VII)

In the experiment involving AgNPs at concentrations of 2, 3, and 4 mg·L $^{-1}$ , significant effects were observed after 30 days of culture for contamination ( $\chi^2$  = 20.75; p < 0.001), explant viability ( $\chi^2$  = 15.38; p = 0.0015), and callus browning ( $\chi^2$  = 25.74; p < 0.001) (Table 8). The 2 mg·L $^{-1}$  treatment resulted in the highest contamination rate, whereas increasing AgNP concentrations progressively reduced this issue. Explant viability increased at 3 and 4 mg·L $^{-1}$ , with the highest performance recorded at 4 mg·L $^{-1}$ . Regarding callus browning, all AgNP treatments significantly decreased the incidence of callus browning compared to the control, indicating a protective effect against tissue oxidation. In contrast, no significant differences were detected for explant oxidation or the frequency of callus formation.

In the experiment VII, which evaluated higher concentrations of AgNPs (4, 8, and 12 mg·L<sup>-1</sup>), only contamination was significantly affected ( $\chi^2 = 8.15$ ; p = 0.043). All AgNP treatments significantly reduced contamination compared to the control, with no statistically significant differences among the tested concentrations (Table 9). However, an increase in tissue losses due to oxidation and a reduction in both callus formation and tissue viability were observed in comparison to the experiment with lower AgNP concentrations.

Forests 2025, 16, 1429 9 of 18

| Table 8. Response of yerba mate leaf explants to different concentrations of silver nanoparticles   |
|---|
| (AgNPs) in terms of contamination, viability, and callus browning after 30 days of in vitro culture |
| (Exp. VI).  |

| Treatment  | Contamination (%) | Oxidation 'ns'<br>(%) | Viable<br>(%) | Callus 'ns'<br>(%) | Oxidized Callus<br>(%) |
|--|-------------------|-----------------------|---------------|--------------------|------------------------|
| Control  | 10.00 a           | 76.70                 | 20.00 a       | 90.00              | 63.30 c                |
| $2 \text{ mg} \cdot \text{L}^{-1} \text{ AgNps}$ | 50.00 b           | 53.30                 | 10.00 a       | 76.70              | 16.70 ab               |
| $3 \text{ mg} \cdot \text{L}^{-1} \text{ AgNPs}$ | 13.30 a           | 63.30                 | 26.70 a       | 83.30              | 43.30 b                |
| $4 \text{ mg} \cdot \text{L}^{-1} \text{ AgNps}$ | 6.70 a            | 43.30                 | 53.30 b       | 86.70              | 10.00 a                |

Orthogonal comparisons among treatments. Different letters indicate significant differences (p < 0.05) based on adjusted orthogonal contrast tests. Odds ratios and standard error values provided in Supplementary Materials. 'ns'—not statistically different.

**Table 9.** Effect of higher concentrations of silver nanoparticles (AgNPs) on contamination, oxidation, viability, and callus formation in leaf explants of yerba mate after 30 days of in vitro culture (Exp. VII).

| Treatment   | Contamination (%) | Oxidation 'ns' (%) | Viable 'ns'<br>(%) | Callus 'ns' (%) |
|---|-------------------|--------------------|--------------------|-----------------|
| Control   | 28.80 b           | 63.50              | 30.80              | 25.00           |
| $4 \text{ mg} \cdot \text{L}^{-1} \text{ AgNps}$  | 13.50 a           | 67.30              | 32.70              | 13.50           |
| $8 \text{ mg} \cdot \text{L}^{-1} \text{ AgNps}$  | 9.80 a            | 47.10              | 52.90              | 11.80           |
| $12 \text{ mg} \cdot \text{L}^{-1} \text{ AgNps}$ | 11.50 a           | 67.30              | 30.8               | 13.50           |

Orthogonal comparisons among treatments. Different letters indicate significant differences (p < 0.05) based on adjusted orthogonal contrast tests. Odds ratios and standard error values provided in Supplementary Materials. 'ns'—not statistically different.

#### 3.6. Effect of Nanoparticles and Growth Regulators on Callogenesis (Experiment VIII)

After 60 days of cultivation, the combination of silver nanoparticles (AgNPs) and growth regulators significantly influenced callus formation in leaf explants of yerba mate (Table 10). The Firth-corrected logistic regression model revealed a highly significant effect of the treatments on callogenesis ( $\chi^2 = 28.09$ ; p < 0.001), with the highest frequencies observed in the combinations of ZEA + 6 mg·L<sup>-1</sup> and BAP + 4 mg·L<sup>-1</sup> AgNPs. In contrast, no statistically significant differences were detected among treatments for overall viability ( $\chi^2 = 7.28$ ; p = 0.2961), oxidation ( $\chi^2 = 10.53$ ; p = 0.1042), or contamination ( $\chi^2 = 6.25$ ; p = 0.3958), although ZEA-based treatments tended to reduce oxidative damage. The treatment with 8 mg·L<sup>-1</sup> BAP was excluded from the statistical analyses due to a high level of contamination, which could bias the interpretation of the results. The elevated explant loss in this group prevented a reliable assessment of the analyzed variables.

Regarding internodal segments, after 60 days on culture, the treatments significantly affected all variables evaluated (Table 11). Contamination ( $\chi^2=37.39;\ p<0.001$ ) was significantly higher in cultures supplemented with BAP and AgNPs than in those containing BAP alone or zeatin, irrespective of the presence of AgNPs. Oxidation ( $\chi^2=22.89;\ p=0.00178$ ) was also more pronounced in BAP treatments, particularly at higher AgNPs concentrations. Viability ( $\chi^2=25.68;\ p=0.0005$ ) and callus formation ( $\chi^2=25.42;\ p=0.0006$ ) were significantly reduced in BAP + AgNPs combinations, especially at 6 and 8 mg·L<sup>-1</sup> of AgNPs.

Forests 2025, 16, 1429 10 of 18

| Table 10. Response of yerba mate leaf explants to combinations of silver nanoparticles (AgNPs) with |
|---|
| BAP or zeatin (ZEA) in terms of contamination, oxidation, viability, and callus formation after 6   |
| days of in vitro culture (Exp. VIII).   |

| Treatment        |  | Contamination 'ns' (%) | Oxidized 'ns' (%) | Viable 'ns' (%) | Callus (%)         |
|------------------|--|------------------------|-------------------|-----------------|--------------------|
|                  | $0 \text{ mg} \cdot L^{-1} \text{ AgNps}$        | 40.00                  | 40.00             | 60.00           | 0.00 b             |
| ZEA              | $4 \text{ mg} \cdot \text{L}^{-1} \text{ AgNps}$ | 35.00                  | 30.00             | 65.00           | $0.00  \mathrm{b}$ |
| (4.56 μM)        | $6 \text{ mg} \cdot \text{L}^{-1} \text{ AgNps}$ | 19.00                  | 19.00             | 66.70           | 38.10 a            |
|                  | $8 \text{ mg} \cdot \text{L}^{-1} \text{ AgNps}$ | 35.00                  | 55.00             | 35.00           | 15.00 a            |
| BAP<br>(4.44 μM) | 0 mg·L <sup>-1</sup> AgNps                       | 25.00                  | 60.00             | 40.00           | 0.00 b             |
|                  | $4 \text{ mg} \cdot \text{L}^{-1} \text{ AgNps}$ | 14.30                  | 42.90             | 57.10           | 42.90 a            |
|                  | $6 \text{ mg} \cdot \text{L}^{-1} \text{ AgNps}$ | 19.00                  | 47.60             | 52.40           | 19.00 a            |

Orthogonal comparisons among treatments. Different letters indicate significant differences (p < 0.05) based on adjusted orthogonal contrast tests. Odds ratios and standard error values provided in Supplementary Materials. 'ns'—not statistically different.

**Table 11.** Response of yerba mate internodal explants to combinations of silver nanoparticles (AgNPs) with BAP or zeatin (ZEA) in terms of contamination, oxidation, viability, and callus formation after 60 days of in vitro culture (Exp. VIII).

| Treatment        |  | Contamination (%) | Oxidized (%) | Viable (%) | Callus (%) |
|------------------|--|-------------------|--------------|------------|------------|
| ZEA<br>(4.56 μM) | 0 mg·L <sup>-1</sup> AgNps                       | 32.30 a           | 54.80 a      | 29.00 a    | 25.80 a    |
|                  | $4 \text{ mg} \cdot \text{L}^{-1} \text{ AgNps}$ | 43.30 a           | 63.30 a      | 33.30 a    | 16.70 a    |
|                  | $6 \text{ mg} \cdot \text{L}^{-1} \text{ AgNps}$ | 35.50 a           | 71.00 a      | 22.60 ab   | 22.60 a    |
|                  | $8 \text{ mg} \cdot \text{L}^{-1} \text{ AgNps}$ | 40.00 a           | 80.00 ab     | 16.70 ab   | 16.70 a    |
| BAP<br>(4.44 μM) | 0 mg·L <sup>-1</sup> AgNps                       | 30.00 a           | 73.30 ab     | 23.30 ab   | 20.00 a    |
|                  | $4 \text{ mg} \cdot \text{L}^{-1} \text{ AgNps}$ | 76.70 bc          | 86.70 ab     | 0.00  b    | 0.00 b     |
|                  | $6 \text{ mg} \cdot \text{L}^{-1} \text{ AgNps}$ | 56.70 ab          | 96.70 b      | 0.00 b     | 0.00 b     |
|                  | $8 \text{ mg} \cdot \text{L}^{-1} \text{ AgNps}$ | 83.30 c           | 83.30 ab     | 16.70 ab   | 0.00 b     |

Orthogonal comparisons among treatments. Different letters indicate significant differences (p < 0.05) based on adjusted orthogonal contrast tests. Odds ratios and standard error values provided in Supplementary Materials.

#### 3.7. Characterization of Callus Morphology

The morphological characteristics of the calli transferred to the differentiation media are shown in Figure 2. The calli originated from leaf and internode explants across all treatments in Experiments VI, VIII, VIII. None of the treatments induced evident embryogenic differentiation; however, distinct callus morphologies were observed within the same treatment.

In treatment 2,4-D 4.53  $\mu$ M + BAP 16  $\mu$ M, the calli presented exhibited colors ranging from yellowish–green (Figure 2c) to dark brown (Figure 2d). The texture as compact (Figure 2c,d) with a nodular appearance, with low friability. In treatment 2,4-D 2.27  $\mu$ M + BAP 8  $\mu$ M, the calli appeared more homogeneous and voluminous with predominant yellowish-green coloration (Figure 2c), with some translucent areas (Figure 2a). The texture was less compact than in 2,4-D 4.53  $\mu$ M + BAP 16  $\mu$ M, showing some friability and granularity (Figure 2a).

In treatment 2,4-D 4.53  $\mu$ M + KIN 17  $\mu$ M, resulted in variable morphologies: shows rounded, crystalline structures (Figure 2b); gelatinous texture (Figure 2a) and presented a granular structure with yellowish-green coloration (Figure 2c). In treatment 2,4-D 2.27  $\mu$ M + KIN 8.5  $\mu$ M, the calli were most compact and intensely colored, yellowish–green (Figure 2c) to dark brown (Figure 2d), also gelatinous surfaces with low friability and dense organization.

Forests 2025, 16, 1429 11 of 18

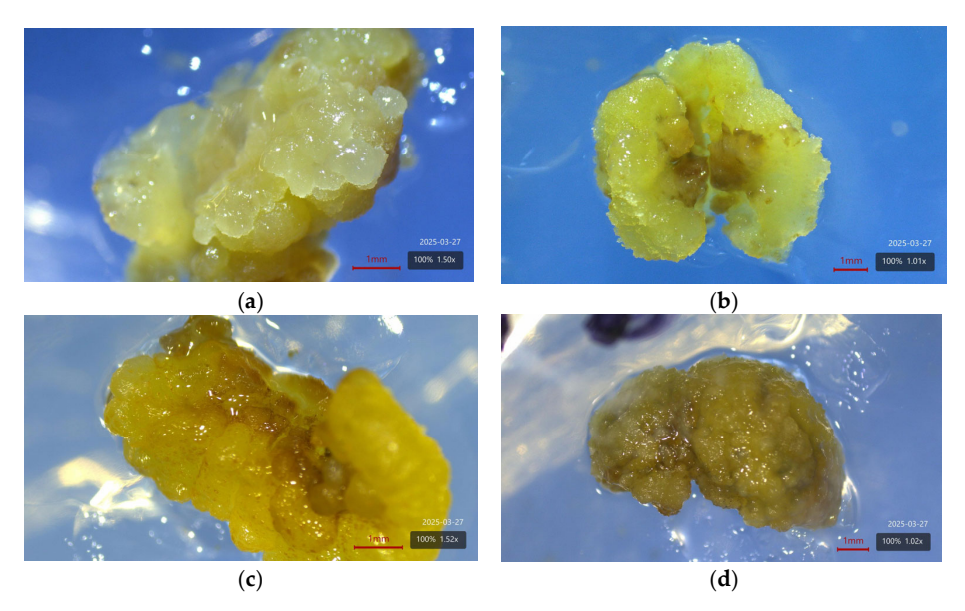


**Figure 2.** Representative images of morphologies of calli induced from leaf explants under different PGR treatments after 60 days of in vitro culture. Treatments and corresponding images: (a) 2,4-D 2.27  $\mu$ M + BAP 8  $\mu$ M; (b,d) 2,4-D 4.53  $\mu$ M + BAP 16  $\mu$ M; (c) 2,4-D 4.53  $\mu$ M + kinetin 17.

#### 3.8. Characterization of Silver and Chitosan Nanopowders

Dynamic light scattering analysis revealed that silver nanopowder (AgNPs, Sigma-Aldrich) at 25 mg·L $^{-1}$  showed an average hydrodynamic diameter of 202.3 nm with a polydispersity index (PDI) of 0.291, indicating moderate size distribution. In comparison, chitosan nanopowder (ChNPs, Quitomax Indústria e Comércio Ltda.) at 60 mg·L $^{-1}$  showed a smaller average diameter of 104.8 nm but showed higher heterogeneity (PDI = 0.412).

Zeta potential measurements indicated limited coloidal stability for both nanoparticles' types, with AgNPs showing slightly positive values (+1.9 mV) and ChNPs slightly negative values (-1.3 mV). This proximity of these values to the neutral point suggest weak electrostatic stabilization and increased aggregation tendency in aqueous suspensions. Scanning electron microscopy (SEM) confirmed predominantly spherical particles for AgNPs (Figure 3a), while ChNPs exhibited irregular and highly polydisperse shapes (Figure 3b). Both samples showed visible particle aggregation observed tendency (Figure 3a,b), corroborating the limited stability inferred from zeta potential data.

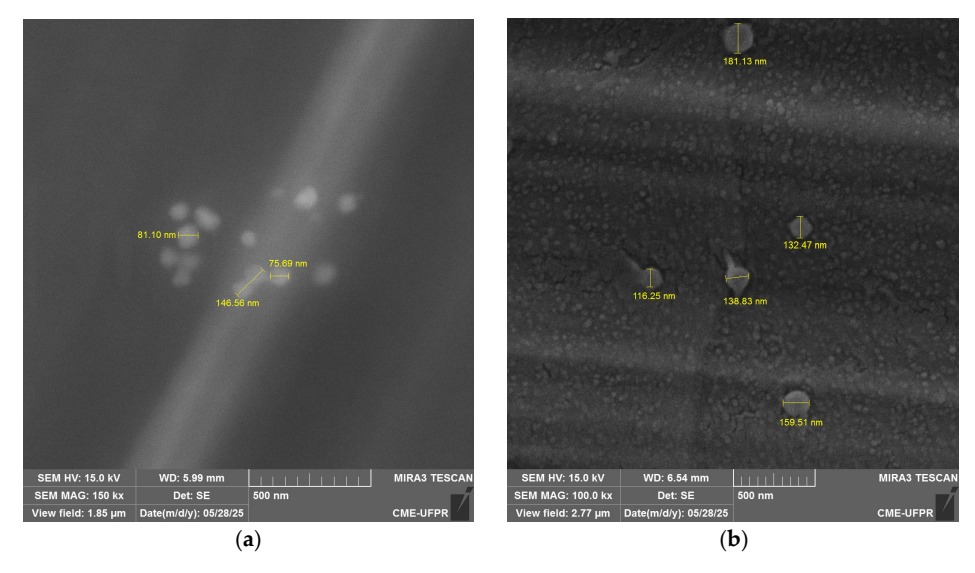


**Figure 3.** Scanning electron microscopy (SEM) of silver nanoparticles (**a**) and chitosan nanoparticles (**b**), illustrating morphology, polydispersity, and aggregation.

Forests 2025, 16, 1429

# 4. Discussion

In vitro culture of yerba mate presents notable challenges, largely due to the recurring presence of endophytic bacteria that persist even after successive subcultures, hindering the establishment of axenic cultures [11,12]. In this context, silver nanoparticles (AgNPs) have emerged as a promising alternative to conventional disinfectants.

The promising results obtained for nodal segments in yerba mate (Experiment I) align with previous studies that investigated silver nanoparticles (AgNPs) as pre-disinfection agents in other species. In the present study, immersion in 1% colloidal silver solution for 20 min reduced contamination to 17.2%, while maintaining tissue viability at 62.1%, proving more effective than the tested fungicide and comparable to chlorhexidine (0.2%–2%). Similarly, Pastelín-Solano et al. [34] observed that immersion of nodal segments of *Vanilla planifolia* Andrews in 100 mg·L<sup>-1</sup> AgNPs for 20 min reduced contamination to 16.6%, with high viability and no visible phytotoxicity. In *Phoenix dactylifera* L., El-Sharabasy et al. [35] demonstrated that immersion of shoot tip explants—including nodal regions—for 30 min in 5 mg·L<sup>-1</sup> AgNPs resulted in 88.89% survival, only 11.11% contamination, and no mortality.

In leaf explants of yerba mate (Experiment IV), the same 1% colloidal silver solution for 20 min yielded the lowest contamination rate (15%) and the lowest oxidation index (35%) among all treatments, contrasting with protocols using sodium hypochlorite or shorter exposure times. Despite the known sensitivity of leaf tissues to oxidative stress, no significant phytotoxicity was observed under this condition. Applied studies reinforce this pattern, Tung et al. [18] reported minimal contamination (3.3%) and high survival (96.7%) in strawberry leaves treated with 200 mg·L $^{-1}$  AgNPs for 20 min. While Tung et al. [36] found that treatment of chrysanthemum leaves with 250 mg·L $^{-1}$  AgNPs for 20 min led to the lowest contamination rate and the highest callus induction, surpassing sodium hypochlorite-based protocols.

Overall, these findings reaffirm that the antimicrobial efficacy and safety of AgNPs in in vitro disinfection are highly dependent on nanoparticle concentration, exposure time, explant type, and application method [21]. The reduction in microbial contamination observed in the present study can be attributed to the main mechanisms of action of AgNPs, including disruption of cell wall and membrane integrity, intracellular damage to proteins, lipids, and DNA, and the induction of oxidative stress through ROS generation [21,37]. The release of silver ions further contributes synergistically by impairing enzymatic activity and microbial metabolism, which together explain the efficient disinfection achieved while preserving explant viability, reinforcing the potential of AgNPs as a broad-spectrum disinfectant in plant tissue culture [37]. It is also important to note that, in both Experiments I and IV, a commercial colloidal silver solution (20 ppm) was used, diluted to 1% (final concentration of  $0.2 \, \mathrm{mg} \cdot \mathrm{L}^{-1}$ ), differing from the characterized nanoparticles employed in other phases of this study. This may partially explain the variations observed in effectiveness and tissue response across treatments.

Beyond initial disinfection, another critical limitation in the tissue culture of yerba mate involves phenolic oxidation, particularly in leaf explants. This browning is primarily caused by the activity of polyphenol oxidases (PPOs), which catalyze the oxidation of phenolic substrates to quinones. These quinones readily undergo non-enzymatic polymerization, forming dark pigments that accumulate in the tissues. As highlighted by [38], this process is triggered when cellular compartmentalization is disrupted during explant excision, allowing vacuolar phenolics to interact with plastid-localized PPOs. The resulting oxidized products not only cause visible browning but also exert cytotoxic effects that impair cellular metabolism and compromise explant viability [38].

To mitigate this oxidative stress, the present study evaluated the use of ethylene-inhibiting compounds, including silver nitrate ( $AgNO_3$ ), sodium thiosulfate (ST), and

Forests 2025, 16, 1429 13 of 18

silver thiosulfate (STS) in Experiment V. These compounds act by interfering with ethylene biosynthesis or perception, which is a key pathway associated with tissue senescence and oxidative damage in vitro. Silver ions released from AgNO<sub>3</sub> or STS can block ethylene signaling, thereby reducing stress responses and improving explant viability. ST, in addition to its role in complexing silver, may also contribute to stress alleviation through its antioxidant properties [39]. Although no significant differences were observed among treatments in terms of contamination, explant viability, callus induction, or oxidation index, a significant reduction in callus browning was detected in the antioxidant treatments compared to the control. Notably, the control group showed 20.7% of browned calli, whereas AgNO<sub>3</sub>-, STS-, and ST-treated explants ranged from 0 to 6.7%.

These findings align with those of Bashir et al. [40], who reported that supplementation with 40  $\mu$ M AgNO<sub>3</sub> significantly enhanced embryogenic callus formation and somatic embryo production from zygotic embryo-derived calli of olive (cv. Leccino). Under ethylene-inhibited conditions, AgNO<sub>3</sub> promoted the development of well-formed somatic embryos, highlighting its stimulatory role in olive somatic embryogenesis. Similarly, Sarropoulou et al. [41], demonstrated that silver-based ethylene inhibitors (AgNO<sub>3</sub> and Ag<sub>2</sub>SO<sub>4</sub>) reduced leaf chlorophyll degradation and increased proline accumulation in cherry rootstocks, even in the absence of improved morphogenic responses. These biochemical changes are indicative of stress alleviation and improved physiological status, despite limited rooting or shoot multiplication in some genotypes. Collectively, these studies support the interpretation that the lower browning frequency observed in the present work is associated with the inhibition of ethylene action by the tested compounds, reinforcing their applicability as effective additives for oxidative browning control in in vitro cultures.

In addition to evaluating ethylene inhibitors, this study investigated the incorporation of nanoparticles into the culture medium and their effects on nodal explants of yerba mate. In Experiment II, the application of silver nanoparticles (AgNPs, 202.3 nm) and chitosan nanoparticles (ChNPs, 104.8 nm) at relatively low concentrations (4 and 7 mg·L $^{-1}$  for AgNPs; 5 and 15 mg·L $^{-1}$  for ChNPs) led to significantly increased contamination rates and reduced tissue viability, suggesting phytotoxicity even at moderate doses. In contrast, Experiment III, which assessed higher concentrations of the same formulations, showed no statistically significant differences across treatments, possibly due to uniform toxicity or nanoparticle aggregation limiting bioavailability.

This pattern is consistent with the literature, which associates colloidal aggregation with reduced cellular uptake and lower apparent nanoparticle toxicity [42]. Aggregation induced by autoclaving, as reported by Timoteo et al. [43], may also explain the lower toxicity observed at higher concentrations. Moreover, variations in pH, ionic strength, and culture medium composition significantly affect the colloidal behavior of nanoparticles [42], compromising their bioavailability and biological activity. In this context, the greater viability observed at 15 mg·L $^{-1}$  of ChNPs suggests that toxicity did not follow a linear dose-dependent response, but was modulated by factors such as colloidal stability and physicochemical interactions with the medium constituents. In *Campomanesia rufa* (O.Berg) Nied., for example, AgNPs at concentrations up to 1.54 mg·L $^{-1}$  were harmless, whereas 15.4 mg·L $^{-1}$  severely inhibited growth without visible anatomical changes [43], indicating the existence of species-specific responses.

This interspecific variation is further supported by reports on other woody species. In *Araucaria excelsa*, the addition of  $400 \text{ mg} \cdot \text{L}^{-1}$  of AgNPs to the culture medium reduced bacterial contamination from 81.25% to 18.75% without causing phytotoxic effects, even at the highest concentrations [20].

Similarly, Abogarra et al. [44] reported that in *Phoenix dactylifera*, the application of  $100 \text{ mg} \cdot \text{L}^{-1}$  of AgNO<sub>3</sub>-NPs and ChNPs stimulated regeneration, while higher concen-

Forests 2025, 16, 1429 14 of 18

trations impaired growth, indicating a dose-sensitive response. Along the same lines Darwesh et al. [45], demonstrated that AgNPs (5–10 mg·L $^{-1}$ ) favored the development of *Olea europaea* L. and reduced microbial contamination, while ChNPs (up to 40 mg·L $^{-1}$ ) induced negative impact on the growth behavior and multiplication of olive shoots grown in vitro.

In this regard, Johnson et al. [46], emphasize that environmental changes can destabilize functionalized nanoparticles, promoting their aggregation and sedimentation, supporting the hypothesis that colloidal instability may have compromised the effectiveness of AgNPs and ChNPs in the in vitro culture of yerba mate.

Experiments VI and VII demonstrated a biphasic response to AgNPs, particularly at 4 mg·L<sup>-1</sup> produced more favorable outcomes, which reduced microbial contamination and increased tissue viability. However, higher concentrations did not differ from the 4 mg/L treatment, indicating no additional benefit in antimicrobial activity. Similar biphasic responses have been reported in Alfarraj et al. [47] *Rumex nervosus* Vahl, explants cultured in media supplemented with biosynthesized AgNPs showed significantly increased callus growth at 40 mg·L<sup>-1</sup>, the highest dose tested, while lower concentrations were less effective. Likewise, in *Panax vietnamensis* Ha & Grushv., AgNPs enhanced somatic embryogenesis and morphogenesis of leaf-derived callus at 1.6 mg·L<sup>-1</sup>, but growth declined at higher doses, likely due to increased oxidative stress and ethylene accumulation [48].

Mechanistically, the phytotoxic effects of silver nanoparticles have been attributed to multiple interrelated pathways, including silver ion (Ag<sup>+</sup>) release, overproduction of reactive oxygen species (ROS), and destabilization of cellular membranes. These processes compromise membrane integrity, disrupt redox homeostasis, and interfere with vital cellular components such as DNA and proteins [21].

Building upon these observations, Experiment VIII further demonstrated that the biological response to AgNPs is not only dose-dependent but also significantly influenced by the presence of growth regulators such as zeatin (ZEA) and benzylaminopurine (BAP) and also type of explant. In leaf explants, combinations with 4–6 mg·L $^{-1}$  AgNPs led to a significant increase in callus formation when associated with either BAP or ZEA, without negatively affecting viability. The combination of ZEA + 6 mg·L $^{-1}$  AgNPs resulted in 38.1% callus formation, while BAP + 4 mg·L $^{-1}$  AgNPs reached 42.9%.

In internodal segments, combinations with BAP and AgNPs inhibited callus formation and reduced viability. In contrast, combinations with zeatin promoted callus formation, maintained viability, and reduced oxidation. These results demonstrate that the choice of both cytokinin and explant type is critical for mitigating the toxic effects of AgNPs.

This interaction might be related to the differential influence of cytokinins on cellular physiology and oxidative metabolism. Silver nanoparticles (AgNPs) can induce the generation of reactive oxygen species (ROS), which can damage membranes, proteins, and DNA [21]. BAP, by stimulating phenylpropanoid metabolism, can enhance the production of phenolic compounds and the antioxidant response, which, when combined with AgNPs, might lead to increased ROS accumulation and exacerbation of oxidative stress [46]. In contrast, zeatin has been associated with greater tolerance to abiotic stresses such as salinity, cold, and heavy metals, by modulating photosynthesis, preserving cell membrane integrity, and stimulating antioxidant enzymes such as catalase (CAT), ascorbate peroxidase (APX), and superoxide dismutase (SOD) [49–51]. These effects might explain the improved physiological performance observed in treatments combining zeatin with AgNPs.

The different combinations of growth regulators directly influenced the morphology of leaf-derived calli in yerba mate, although no treatment induced visible signs of morphogenic differentiation. In treatments with 2,4-D 4.53  $\mu$ M + BAP 16  $\mu$ M (T1) and 2,4-D 4.53  $\mu$ M+

Forests 2025, 16, 1429 15 of 18

KIN 17  $\mu$ M (T4), the calli appeared compact, darkened, and exhibited low friability, these characteristics are consistent with previous descriptions of regeneration-refractory calli [52,53]. Conversely, treatments such as 2,4-D 2.27  $\mu$ M + BAP 8  $\mu$ M (T2) and 2,4-D 2.27  $\mu$ M + KIN 8.5  $\mu$ M (T3) produced more friable and lighter-colored calli, suggesting a more favorable cellular organization, although still lacking morphogenic potential.

Comparable results were observed in *Ilex aquifolium* L., where cytokinin–auxin combinations (notably BAP with NAA or 2,4-D) promoted efficient callus formation characterized by compact texture and varying coloration, although no morphogenic differentiation was reported under the tested conditions [54]. In yerba mate, comparable results were obtained by various authors using leaf explants, with frequent formation of viable yet non-differentiated calli [52–55]. These findings reinforce the strong dependence of the species on hormonal balance and culture conditions to enable morphogenic progression, and suggest that callus viability alone is not a reliable indicator of regeneration potential.

# 5. Conclusions

The in vitro culture of yerba mate faces persistent challenges, particularly due to microbial contamination and oxidative stress, issues that can be mitigated through the use of silver nanoparticles (AgNPs) as pre-disinfection agents. The effectiveness of AgNPs depends on their formulation, explant type, and interaction with cytokinins. Ethylene inhibitors reduced callus browning in leaf explants, zeatin outperformed BAP for nodal explants, and the combination of BAP and AgNPs promoted callogenesis without morphogenesis. In summary, these results demonstrate the promising potential of AgNPs, but future investigations should incorporate culture media enriched with antioxidant compounds, as well as analyses using molecular markers, to maximize the morphogenic competence of yerba mate in vitro cultures.

**Supplementary Materials:** The following supporting information can be downloaded at https://www.mdpi.com/article/10.3390/f16091429/s1.

**Author Contributions:** B.Z.P. conducted the experiments, performed statistical analyses, and wrote the manuscript. J.D. and R.C.Q. conceived and designed the study and contributed to manuscript revision. I.W. supervised the study, provided critical feedback, and contributed to manuscript preparation. All authors have read and agreed to the published version of the manuscript.

**Funding:** This study was supported by the National Council for Scientific and Technological Development (CNPq, grant number 405046/2021-9), the Brazilian Agricultural Research Corporation (Embrapa) and the Coordination for the Improvement of Higher Education Personnel (CAPES—Finance Code 001, grant number 88887.985112/2024-00). The Graduate Program in Forest Engineering of the Federal University of Paraná (UFPR) provided additional support.

**Data Availability Statement:** The data generated and analyzed during this study are available from the corresponding author upon reasonable request.

**Acknowledgments:** The authors thank the staff of the Biopolymers Laboratory and the Electron Microscopy Center at UFPR for their technical assistance. The authors are especially grateful to Washington Luiz Esteves Magalhães (Embrapa Forestry) for providing the chitosan nanoparticles used in this study. Bruna Zanatta Pereira acknowledges her master's scholarship from CAPES. The authors also acknowledge OpenAI's ChatGPT (version GPT-4) for language editing assistance during manuscript preparation. We also thank the anonymous reviewers.

Conflicts of Interest: Authors Regina Caetano Quisen, Juliana Degenhardt and Ivar Wendling were employed by the company Embrapa Forestry. The remaining author declares that the research was conducted in the absence of any commercial or financial relationships that could be construed as a potential conflict of interest.

Forests 2025, 16, 1429 16 of 18

#### **Abbreviations**

The following abbreviations are used in this manuscript:

2,4-D 2,4-Dichlorophenoxyacetic Acid

AgNO<sub>3</sub> Silver nitrate

AgNPS Silver Nanoparticles
BAP 6-Benzylaminopurine
ChNPS Chitosan Nanoparticles
DLS Dynamic Light Scattering
GLMs Generalized Linear Models

KIN Cytokinin

MS Murashige and Skoog NAA 1-Naphthaleneacetic acid PVP Polyvinylpyrrolidone

SEM Scanning Electron Microscopy

ST Sodium Thiosulfate STS Silver thiosulfate

ZEA Zeatin

#### References

1. Gawron-Gzella, A.; Chanaj-Kaczmarek, J.; Cielecka-Piontek, J. Yerba mate—A long but current history. *Nutrients* **2021**, *13*, 3706. [CrossRef]

- 2. FAO—Food and Agriculture Organization of the United Nations. FAOSTAT—Crops and Livestock Products. Available online: https://www.fao.org/faostat (accessed on 10 April 2025).
- 3. Gerber, M.R.; Nunes, A.; Moreira, B.R.; Maraschin, M. Yerba mate (*Ilex paraguariensis* A. St.-Hil.) for new therapeutic and nutraceutical interventions: A review of patents issued in the last 20 years (2000–2020). *Phytother. Res.* **2023**, *37*, 527–548. [CrossRef]
- 4. Rząsa-Duran, M.; Kryczyk-Poprawa, A.; Drabicki, D.; Podkowa, A.; Sułkowska-Ziaja, K.; Szewczyk, A.; Kała, K.; Opoka, W.; Zięba, P.; Fidurski, M.; et al. Yerba mate as a source of elements and bioactive compounds with antioxidant activity. *Antioxidants* **2022**, *11*, 371. [CrossRef] [PubMed]
- 5. Xavier, A.; Wendling, I.; Silva, R.L. Silvicultura Clonal: Princípios e Técnicas, 2nd ed.; UFV: Viçosa, Brazil, 2013.
- 6. Wendling, I.; Santin, D. Propagação e Nutrição de Erva-Mate; Embrapa: Brasília, Brazil, 2015.
- 7. Pimentel, N.; Gazzana, D.; Spanevello, J.F.; Lencina, K.H.; Bisognin, D.A. Effect of mini-cutting size on adventitious rooting and morphophysiological quality *of Ilex paraguariensis* plantlets. *J. For. Res.* **2020**, *32*, 815–822. [CrossRef]
- 8. Duarte, G.O.; Wendling, I.; Bianchini, F.G.; Brondani, G.E. Seasonality and genotype influence on Ilex paraguariensis cuttings rooting and bioactive compounds. *Pesqui. Agropecu. Bras.* **2023**, *58*, 174–181. [CrossRef]
- 9. George, E.F.; Hall, M.A.; De Klerk, G.J. Plant tissue culture procedure—Background. In *Plant Propagation by Tissue Culture*, 3rd ed.; George, E.F., Hall, M.A., De Klerk, G.J., Eds.; Springer: Dordrecht, The Netherlands, 2008; pp. 1–28.
- 10. Gupta, N.; Jain, V.; Joseph, M.R.; Devi, S. A review on micropropagation culture method. *Asian J. Pharm. Res. Dev.* **2020**, *8*, 86–93. [CrossRef]
- Luna, C.; Acevedo, R.; Collavino, M.; González, A.; Mroginski, L.; Sansberro, P. Endophytic bacteria from *Ilex paraguariensis* shoot cultures: Localization, characterization, and response to isothiazolone biocides. *Vitr. Cell. Dev. Biol. Plant* 2013, 49, 326–332. [CrossRef]
- 12. Tomasi, J.C.; Degenhardt-Goldbach, J.; Grunennvaldt, R.L.; dos Santos, G.D.; Vicente, V.A.; Franciscon, L.; Bona, C.; Quiorin, M. In vitro establishment of shoot meristems of *Ilex paraguariensis* and identification of endophytic bacteria. *J. For. Res.* **2019**, *30*, 1765–1777. [CrossRef]
- 13. Liu, C.; Fan, H.; Zhang, J.; Wu, J.; Zhou, M.; Cao, F.; Tao, G.; Zhou, X. Combating browning: Mechanisms and management strategies in in vitro culture of economic woody plants. *For. Res.* **2024**, *4*, e032. [CrossRef]
- 14. Dutra, L.F.; Hansel, F.A.; Wendling, I. *Introdução ao Cultivo In Vitro de Erva-Mate (Ilex paraguariensis)*; Embrapa Florestas: Colombo, Brazil, 2008; p. 38.
- 15. Rey, H.Y.; Sansberro, P.A.; Collavino, M.M.; Daviña, J.R.; González, A.M.; Mroginski, L.A. Colchicine, trifluralin, and oryzalin development of somatic embryos in *Ilex paraguariensis* (*Aquifoliaceae*). *Euphytica* **2002**, 123, 49–56. [CrossRef]
- 16. Elsahhar, S.; Shahba, M.; Elsayed, T.; Mikhail, M.; Galal, A. Effect of Chitosan Nanoparticles (CS-NPs) on In Vitro Regeneration Response and Production of Potato virus Y (PVY)-Free Plants of Potato. *Agronomy* **2022**, *12*, 2901. [CrossRef]

Forests 2025, 16, 1429 17 of 18

17. Mancilla-Álvarez, E.; Serrano-Fuentes, M.K.; Fuentes-Torres, M.A.; Sánchez-Páez, R.; Bello-Bello, J.J. Chitosan Nanoparticles: An Alternative for In Vitro Multiplication of Sugarcane (*Saccharum* spp.) in Semi-Automated Bioreactors. *Plants* **2025**, *14*, 1697. [CrossRef] [PubMed]

- 18. Tung, H.T.; Thuong, T.T.; Cuong, D.M.; Luan, V.Q.; Hien, V.T.; Hieu, T.; Nam, N.B.; Phuong, H.T.N.; Vinh, B.V.T.; Khai, H.D.; et al. Silver nanoparticles improved explant disinfection, in vitro growth, runner formation and limited ethylene accumulation during micropropagation of strawberry (*Fragaria* × *ananassa*). *Plant Cell Tiss. Organ Cult.* **2021**, *145*, 393–403. [CrossRef]
- 19. Jadczak, P.; Kulpa, D.; Bihun, M.; Przewodowski, W. Positive effect of AgNPs and AuNPs in in vitro cultures of Lavandula angustifolia Mill. *Plant Cell Tiss. Organ Cult.* **2019**, 139, 191–197. [CrossRef]
- 20. Sarmast, M.K.; Salehi, H.; Khosh-Khui, M. Nano silver treatment is effective in reducing bacterial contaminations of *Araucaria excel* R. Br. var. *Glauca* explants. *Biol. Futur.* **2011**, *62*, 477–484.
- 21. Dakal, T.C.; Kumar, A.; Majumdar, R.S.; Yadav, V. Mechanistic basis of antimicrobial actions of silver nanoparticles. *Front. Microbiol.* **2016**, *7*, 1831. [CrossRef]
- 22. Ke, C.; Deng, F.; Chuang, C.; Lin, C. Antimicrobial Actions and Applications of Chitosan. Polymers 2021, 13, 904. [CrossRef]
- 23. Balamurugan, V.; Abdi, G.; Karthiksaran, C.; Thillaigovindhan, N.; Thillaigovindhan, D. A review: Improvement of plant tissue culture applications by using nanoparticles. *J. Nanopart. Res.* **2024**, *26*, 188. [CrossRef]
- 24. Alves, H.J.; Vieceli, M.; Alves, C.; Muñiz, G.I.; de Oliveira, C.L.; Feroldi, M.; Arantes, M.K. Chitosan depolymerization and nanochitosan production using a single physical procedure. *J. Polym. Environ.* **2018**, *26*, 3913–3923. [CrossRef]
- 25. Alves, H.J.; Gasparrini, L.J.; Bueno Silva, F.E.; Caciano, L.; Bolzon de Muniz, G.I.; Cupertino Ballester, E.L.; Cremonez, P.A.; Arantes, M.A. Alternative methods for the pilot-scale production and characterization of chitosan nanoparticles. *Environ. Sci. Pollut. Res.* **2021**, *28*, 10977–10987. [CrossRef]
- 26. Oliveira, K.M.G.; Moura, R.B.P.; Taveira, S.F.; Zielonka, H.L.; Brum, D.O.; Silva, E.Z.M.; Trindade, E.S.; Cestari, M.M.; Cademartori, P.H.G.; Magalhães, W.L.E.; et al. Exploring the applicability of the RTgill-W1 and ZFL cell line assays in aquatic hazard assessment of mineral and organic nanomaterials. *Chemosphere* 2025, 386, 144617. [CrossRef]
- 27. Murashige, T.; Skoog, F. A revised medium for rapid growth and bioassays with tobacco tissue cultures. *Physiol. Plant.* **1962**, *15*, 473–497. [CrossRef]
- 28. McCullagh, P.; Nelder, J.A. Generalized Linear Models, 2nd ed.; Chapman and Hall: London, UK, 1989. [CrossRef]
- 29. Fox, J.; Weisberg, S. An R Companion to Applied Regression, 3rd ed.; Sage: Thousand Oaks, CA, USA, 2019.
- 30. Firth, D. Bias reduction of maximum likelihood estimates. Biometrika 1993, 80, 27–38. [CrossRef]
- 31. Altman, D.G. Practical Statistics for Medical Research; Chapman and Hall: London, UK, 1991.
- 32. Piepho, H.P. An algorithm for a letter-based representation of all-pairwise comparisons. *J. Comput. Graph. Stat.* **2004**, *13*, 456–468. [CrossRef]
- 33. R Core Team. *R: A Language and Environment for Statistical Computing*; R Foundation for Statistical Computing: Vienna, Austria, 2024; Available online: https://www.r-project.org (accessed on 10 April 2025).
- 34. Pastelín-Solano, M.C.; Ramírez-Mosqueda, M.A.; Bogdanchikova, N.; Castro, C.; Bello-Bello, J.J. Silver nanoparticles affect the micropropagation of vanilla (*Vanilla planifolia Jacks.* ex Andrews). *Agrociencia* **2020**, *54*, 1–13.
- 35. El-Sharabasy, S.F.; Moustafa, M.F.; Gabr, A.M.; Ghareeb, R.Y. In vitro application of silver nanoparticles as explant disinfectant for date palm cultivar Barhee. *J. Appl. Hortic.* **2017**, *19*, 106–112. [CrossRef]
- 36. Tung, H.T.; Bao, H.G.; Cuong, D.M.; Ngan, H.T.M.; Hien, V.T.; Luan, V.Q.; Vinh, B.V.T.; Phuong, H.T.N.; Nam, N.B.; Trieu, L.N.; et al. Silver nanoparticles as the sterilant in large-scale micropropagation of chrysanthemum. *Vitr. Cell. Dev. Biol. Plant* 2021, 57, 297–309. [CrossRef]
- 37. Abdi, G.; Salehi, H.; Khosh-Khui, M. Nano silver: A novel nanomaterial for removal of bacterial contaminants in valerian (*Valeriana officinalis* L.) tissue culture. *Acta Physiol. Plant.* **2008**, *30*, 709–714. [CrossRef]
- 38. Mayer, A.M. Polyphenol oxidases in plants and fungi: Going places? A review. Phytochemistry 2006, 67, 2318–2331. [CrossRef]
- 39. Binder, B.M.; Schaller, G.E. Ethylene Signaling: Methods and Protocols. Methods Mol. Biol. 2017, 1573, 215–230.
- 40. Bashir, M.A.; Silvestri, C.; Salimonti, A.; Rugini, E.; Cristofori, V.; Zelasco, S. Can ethylene inhibitors enhance the success of olive somatic embryogenesis? *Plants* **2022**, *11*, 168. [CrossRef]
- 41. Sarropoulou, V.; Dimassi-Theriou, K.; Therios, I. Effect of the ethylene inhibitors silver nitrate, silver sulfate, and cobalt chloride on micropropagation and biochemical parameters in the cherry rootstocks CAB-6P and Gisela 6. *Turk. J. Biol.* **2016**, *40*, 670–683. [CrossRef]
- 42. Moore, T.L.; Rodriguez-Lorenzo, L.; Hirsch, V.; Balog, S.; Urban, D.; Jud, C.; Rothen-Rutishauser, B.; Lattuada, M.; Petri-Fink, A. Nanoparticle colloidal stability in cell culture media and impact on cellular interactions. *Chem. Soc. Rev.* **2015**, 44, 6287–6305. [CrossRef] [PubMed]
- 43. Timoteo, C.D.; Paiva, R.; dos Reis, M.V.; Claro, P.I.C.; da Silva, D.P.C.; Marconcini, J.M.; de Oliveira, J.E. Silver nanoparticles in the micropropagation of *Campomanesia rufa* (O. Berg) Nied. *Plant Cell Tiss. Organ Cult.* **2019**, *137*, 359–368. [CrossRef]

Forests 2025, 16, 1429 18 of 18

44. Abogarra, L.; Eisa, N.; El-Habbaa, G.; Darwesh, R.S.; El-Habbak, M. Superiority of nano-silver nitrate and nano-chitosan in controlling bacterial contamination and promoting growth of in vitro date palm cultures. *Plant Cell Biotechnol. Mol. Biol.* **2022**, 23, 85–104. [CrossRef]

- 45. Darwesh, O.M.; Hassan, S.A.M.; Abdallatif, A.M. Improve in vitro multiplication of olive shoots using environmental-safe chitosan, selenium, and silver nanostructures. *Biosci. Rev. Adv. Concepts* **2023**, *13*, 419.
- 46. Johnson, L.; Gray, D.M.; Niezabitowska, E.; McDonald, T.O. Multi-stimuli-responsive aggregation of nanoparticles driven by the manipulation of colloidal stability. *Nanoscale* **2021**, *13*, 7879–7896. [CrossRef]
- 47. Alfarraj, N.S.; Tarroum, M.; Al Qurainy, F.; Nadeem, M.; Khan, S.; Salih, A.M.; Shaikhaldein, H.O.; Al-Hashimi, A.; Alansi, S.; Perveen, K. Biosynthesis of silver nanoparticles and exploring their potential of reducing the contamination of the in vitro culture media and inducing the callus growth of *Rumex nervosus* explants. *Molecules* **2023**, *28*, 3666. [CrossRef]
- 48. Cuong, D.T.; Du, P.C.; Tung, H.T.; Ngan, H.T.M.; Luan, V.Q.; Khai, H.D.; Phuong, T.T.B.; Nhut, D.T. Silver nanoparticles as an effective stimulant in micropropagation of *Panax vietnamensis*—A valuable medicinal plant. *Plant Cell Tiss. Organ Cult.* **2021**, 146, 577–588. [CrossRef]
- 49. Hönig, M.; Plíhalová, L.; Husičková, A.; Nisler, J.; Doležal, K. Role of cytokinins in senescence, antioxidant defence and photosynthesis. *Int. J. Mol. Sci.* **2018**, *19*, 4045. [CrossRef]
- 50. Liu, X.; Huang, B.; Banowetz, G. Cytokinin effects on creeping bentgrass responses to heat stress: I. *Shoot Root Growth. Crop Sci.* **2002**, 42, 457–465.
- 51. Xu, Y.; Huang, B. Effects of foliar-applied ethylene inhibitor and synthetic cytokinin on creeping bentgrass to enhance heat tolerance. *Crop Sci.* **2009**, *49*, 1876. [CrossRef]
- 52. Grunennvaldt, R.L.; Degenhardt-Goldbach, J.; Brooks, P.; Tomasi, J.D.C.; Hansel, F.A.; Tran, T.; Gomes, E.N.; Deschamps, C. Callus culture as a new approach for the production of high added value compounds in *Ilex paraguariensis*: *Genotype* influence, medium optimization and compounds identification. *An. Acad. Bras. Ciênc.* 2020, 92, e20181251. [CrossRef] [PubMed]
- 53. Degenhardt-Goldbach, J.; Stachevski, T.W.; Franciscon, L.; Buss, S.; Wendling, E.; Dutra, L.F. Calogênese in vitro a partir de folhas de erva-mate (*Ilex paraguariensis* St. Hil.) mantidas em casa de vegetação. In Proceedings of the Actas del 5° Congreso Sudamericano de la Yerba Mate, Posadas, Argentina, 5–6 May 2011; INYM: Posadas, Argentina, 2011; pp. 61–66.
- 54. Khater, N.; Benahmed, A.; Zereg, N.; Cherouana, K. Callogenesis induction of *Ilex aquifolium* L. (*Aquifoliaceae*). S. Afr. J. Bot. **2021**, 12, 265–272.
- 55. Stachevski, T.W.; Franciscon, L.; Degenhardt-Goldbach, J. Callus induction in vitro on leaves explants of *Ilex paraguariensi*. *Braz. J. For. Res.* **2013**, 33, 339–342.

**Disclaimer/Publisher's Note:** The statements, opinions and data contained in all publications are solely those of the individual author(s) and contributor(s) and not of MDPI and/or the editor(s). MDPI and/or the editor(s) disclaim responsibility for any injury to people or property resulting from any ideas, methods, instructions or products referred to in the content.